J|A|C|S COMMUNICATIONS

Published on Web 04/06/2009

Shape-Dependent Activity of Platinum Array Catalyst

Vladimir Komanicky,[†,‡,§] Hakim Iddir,[§] Kee-Chul Chang,[§] Andreas Menzel,[§,||] Goran Karapetrov,[§] Daniel Hennessy,[§] Peter Zapol, and Hoydoo You*[,§]

Safarik University, Faculty of Sciences and, Institute of Experimental Physics, SAS, Kosice 04154, Slovakia, Materials Science Division, Argonne National Laboratory, Argonne, Illinois 60439, and Paul Scherrer Institut, 5232 Villigen PSI, Switzerland

Received January 28, 2009; E-mail: vladimir.komanicky@upjs.sk; hyou@anl.gov

Catalysis is an integral part of manufacturing virtually all consumer products and is especially important in addressing the energy-related challenges of the future. However, many catalytic systems are not well understood, including technologically important metal nanoparticle catalysts dispersed on high-surface-area supports. Typically, such catalysts are poorly defined in terms of size, shape, and composition, and characterization of them under realistic conditions remains challenging. Although particle size, surface structure, and the metal−support interfaces are all expected to have a great influence on catalytic activity and selectivity,[1] these microscopic factors have yet to be optimized and controlled. Combining first-principles calculations[2] with nanofabrication techniques is a promising way to design catalyst systems containing millions of identical nanoparticles sufficiently large in number for conventional laboratory measurements.

In this communication, guided by DFT calculations[2] to predict particle shape, we deploy nanofabrication techniques to produce platinum nanoparticle arrays with nearly perfect control of particle number, morphology, position, and orientation. This allows us to relate microscopic morphologies with macroscopic catalytic reactivities, e.g., an oxygen-reduction reaction, the sluggishness of which is impeding widespread deployment of hydrogen fuel cells in the automotive industry. We find increased oxygen reduction activity and attribute it to a cooperative interplay between facets with different affinities to oxygen.

We produced millions of identical platinum nanoparticles with a 30 to 40 nm diameter in ordered arrays on strontium titanate (STO). Three distinctive shapes of nanoparticles could be selected by choice of the substrates' crystallographic orientations and annealing conditions. The arrays were fabricated from epitaxially grown platinum films utilizing electron beam lithography (EBL). They were characterized by scanning electron microscopy (SEM) and synchrotron X-ray scattering (SXS). Since oxygen reduction reaction (ORR) kinetics is widely studied on platinum single-crystal electrodes, and its surface dependencies are well-known,[3] we tested the produced nanoparticle arrays for ORR activities.

An initial set of platinum particle arrays were fabricated by EBL from the films grown by the three-step process[4] on STO(100), (111), and (110) substrates and annealed at 1450 K in a nitrogen flow. SEM images of the resulting platinum particle arrays are shown in Figure 1. Each array consists of $\sim 75 \times 10^6$ particles registered in a square lattice with a 200 nm period. X-ray diffraction measurements (Supporting Information Figure 1) indicate that, in all three cases, the platinum particles form epitaxial structures with the crystallographic orientations of the nanoparticles registered to those of the substrates. Wide-angle reflectivity scans detect no population of misoriented platinum nanoparticles.

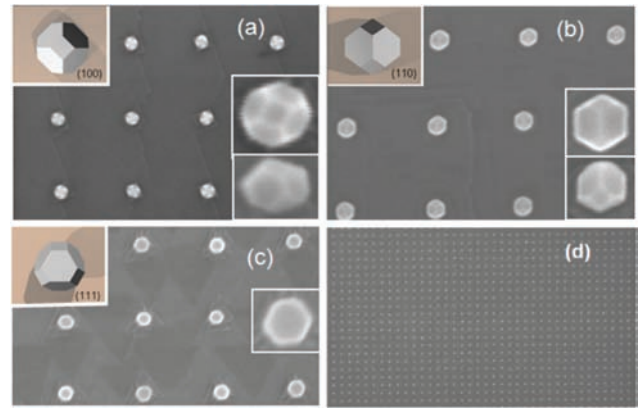

Figure 1. (a−c) SEM images of (100), (110), and (111) arrays, respectively. Insets on the right are close-up top and side views, and insets on the left are the shapes rendered by slicing a cuboctahedron in three directions. Particles are located on 200 nm square lattices. In close examination of the images (a) and (c), square- or triangular-based pyramidal pedestals of STO, created during etching and annealing, can also be seen below the particles. (d) shows a zoomed out view of an array.

As can be seen in Figure 1, the shapes of Pt particles on STO(100) and STO(110) correspond to a cuboctahedron of an ∼30 nm diameter, cut approximately in half, normal to respective planes. In the case of the (111)-oriented substrate, however, particles wet the substrate better and instead form hexagonal platelets. Since the volumes of platinum particles are expected to be similar in all three arrays, (111) epitaxy leads to wider and thinner hexagonal crystals. Electron micrographs indicate a diameter of ∼40 nm, and from the diffraction fringes for nanocrystals from SXS, we determine the height of the particles to be ∼7.5 nm. X-ray crystallography found two equally probable populations of (111) platinum nanoparticles, corresponding to two possible stacking sequences of (111) planes. Other than their stacking sequences, these particles are identical in shape and orientation.

The crystal shapes seen in the arrays can be well explained by partial wetting of platinum on STO in DFT calculations.[2] Since the arrays were annealed in nonadsorbing nitrogen, our DFT calculations took into account only the interfacial energies between STO substrates and platinum with no adsorbed species on the facets. The shapes are also in good agreement with a recent MD study[5] of annealing platinum nanoparticles.

As a traditional macroscopic characterization, we tested oxygen-reduction electrocatalytic activities of the three arrays shown in Figure 1. Current−voltage curves, measured in oxygen-saturated 0.1 M perchloric acid, are shown in Figure 2. In all cases, the activity is kinetically limited at low overpotentials and oxygen-diffusion limited at high overpotentials. Independent of the presence

[†] Safarik University.
[‡] Institute of Experimental Physics, SAS.
[§] Argonne National Laboratory.
[||] Paul Scherrer Institut.

10.1021/ja900459w CCC: $40.75

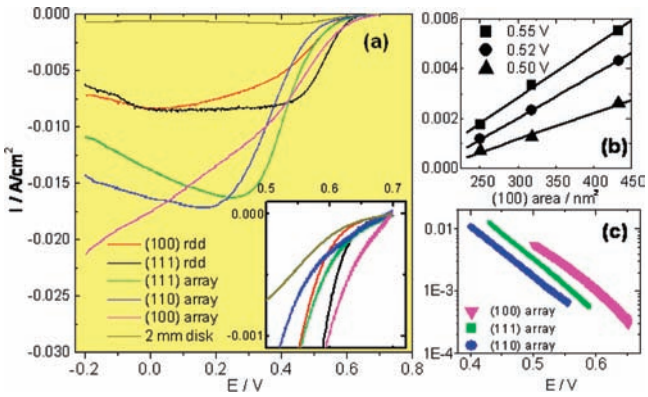

Figure 2. (a) Oxygen reduction current densities. The $I-V$ curves were obtained by sweeping voltage from 0.7 V to −0.2 V at 50 mV/s. Potential scale is reference vs Ag/AgCl electrode. The inset is a close-up view of the data. (b) The kinetic current densities vs area of the (100) surface normalized to the overall particle surface at three selected potentials. Kinetic current densities were obtained using the Levich−Koutecky form. (c) Tafel plots (log of kinetic current densities vs E) of the $I-V$ curves.

of oxygen in the solution, the current−voltage curves measured for the bare STO substrates are essentially flat, with no significant features over the explored potential range.

We used surface areas based on both measurements and theoretical calculations to calculate the current densities for the arrays. The current−voltage response of the 2 mm wide (111)-oriented platinum film evaporated on STO(111) is essentially diffusion limited, except for the very near onset potential (∼0.7 V). Since the diffusion rate of reactants to an array of nanoelectrodes[6] separated by an inactive surface is expected to be much higher, we compared the arrays to more appropriate rotating-disk (RD) data measured for Pt(111) and Pt(100) single-crystal electrodes. The RD data are clearly not diffusion limited in the low overpotential region. At large overpotentials (∼0.3 V), oxygen reduction currents are diffusion-limited, as indicated by the current plateau in the current−voltage curves. As shown in the inset of Figure 2, however, the arrays have high onset potentials and high activity at the kinetic region. Note in particular that the (100) array has an even higher activity than Pt(111), commonly held to have the highest activity.[3]

In the case of platinum single crystals, the higher affinity for oxide species of the (100) surface than for those of the (111) surface results in lower activity.[3] It is therefore remarkable that, at least at the onset potential, the (100) array is far more active than the algebraic average of activities for the (100) and (111) facets. However, we observed similar properties in the case of one-dimensional arrays of alternating (100) and (111) nanofacets[7] formed on single crystal surfaces. We suggest that the increased activity is a general behavior of facets in nanoscale proximity—we call it a "division of labor" between (100) and (111) nanofacets. For example, the (100) facets adsorb oxygen well[8] but cannot reduce efficiently. The (111) facets can reduce oxygen but cannot easily absorb it.[8] The nanoscale proximity may allow oxygen that is adsorbed on (100) to diffuse to the (111) facets, where it can be more efficiently reduced. In this case, the activity of the arrays should increase with the ratio of (100) to (111) surfaces.

Tafel plots shown in Figure 2c suggest the reduction reaction takes place in (111) facets. The Tafel slopes are 126 mV/dec for the (100) array, 119 mV/dec for the (111) array, and 125 mV/dec for the (110) arrays. These are close to the experimentally found values for Pt (111) RD[3,7] and to theoretically calculated value of 118 mV/dec for a single electron transfer reaction. This indicates that the charge-transferring rate-determining step (RDS) could be the same for all three discussed arrays. We can assume that RDS most likely takes place on (111) facets since the currents for (100) RD disks are much lower due to partial surface blocking by oxygenated species.[3,7]

If we assume that the (100) facets simply act as "collectors of oxygen", the linear dependence of kinetic current densities on the (100) facet area can be expected as long as (111) facets can efficiently and dominantly process the reaction. Based on SEM data, we obtain the following ratios: 1:2 for (100)-oriented arrays, 1:3 for (111)-oriented arrays, and 1:4 for (110)-oriented arrays. Corresponding plots of kinetic current densities, which are an inherent measure of activity, at three selected potentials vs the (100) area normalized to the overall particle surface, are shown in Figure 2b. These data indeed show the linear dependency and suggest a (111) facet may process the reaction potentially significantly more if we can supply more oxygen. These simple observations cannot explain all the complexities of the current−voltage curves shown in Figure 2a. Nonetheless it is clear that even identically sized nanoparticles can have different catalytic activities depending on the shapes.

In conclusion, we demonstrated the ability to fabricate perfectly registered and oriented arrays of essentially identical platinum nanoparticles on STO. Depending on the substrate crystallography, three different shapes of nanoparticles were observed. We measured the oxygen reduction reaction activity, one of the most important electrocatalytic activities, and demonstrated its sensitivity to the nanoscale shape of a catalyst particle. Our observation of the unexpectedly high onset potential adds another piece of possible evidence to the concept of "division of labor" between nanoscale facets, previously suggested in the study of nanostructured single-crystal surfaces.[7] Although EBL is a serial technique, which limits our capability to produce large areas covered with catalyst particles, advances in parallel nanofabrication techniques[9] are expected to overcome these limitations, possibly extending our approach to the preparation of industrial catalysts with optimum performance.

Acknowledgment. We thank Leonidas Ocola and Ralu Divan for their help during array nanofabrication. This work and use of the Advanced Photon Source, the Center for Nanoscale Materials and the Electron Microscopy Center for Materials Research were supported by the U.S. Department of Energy, Office of Science, Office of Basic Energy Sciences, under Contract No. DE-AC02-06CH11357.

Supporting Information Available: Experimental details of nanofabrication and X-ray characterization of the arrays. This material is available free of charge via the Internet at http://pubs.acs.org.

References

(1) (a) Narayanan, R.; El-Sayed, M. A. *Nano Lett.* **2004**, *4*, 1343–1348. (b) Arenz, M.; Mayrhofer, K. J. J.; Blizanac, B. B.; Samenkovic, V.; Ross, P. N.; Markovic, N. M. *J. Am. Chem. Soc.* **2005**, *127*, 6819–6829. (c) Tian, N.; Zhou, Z.; Sun, S.; Ding, Y.; Wang, Z. *Science* **2007**, *316*, 732–735.
(2) Iddir, H.; Komanicky, V.; Ogut, S.; Zapol, P.; You, H. *J. Phys. Chem. C* **2007**, *111*, 14782–14789.
(3) Markovic, N. M.; Adzic, R. R.; Cahan, B. D.; Yeager, E. *J. Electroanal. Chem.* **1994**, *377*, 249–259.
(4) Francis, A. J.; Cao, Y.; Salvador, P. A. *Thin Solid Films* **2006**, *496*, 317–325.
(5) Wen, Y.; Fang, H.; Zhu, Z.; Sun, S. *Phys. Lett. A* **2009**, *373*, 272–276.
(6) Reller, H.; Kirowa-Eisner, E.; Gileadi, E. *J. Electroanal. Chem.* **1982**, *138*, 65–77.
(7) Komanicky, V.; Menzel, A.; You, H. *J. Phys. Chem. B* **2005**, *109*, 23550–23557.
(8) Panchenko, A.; Koper, M. T. M.; Shubina, T. E.; Mitchell, S. J.; Rodunera, E. *J. Electrochem. Soc.* **2004**, *151*, A2016−A2027.
(9) Chou, S. Y.; Krauss, P. R.; Renstrom, P. J. *Science* **1996**, *272*, 85–87.

JA900459W